Research article

Irene Estébanez, Janek Schwind, Ingo Fischer and Apostolos Argyris*

Accelerating photonic computing by bandwidth enhancement of a time-delay reservoir

https://doi.org/10.1515/nanoph-2020-0184
Received March 9, 2020; accepted May 6, 2020; published online June 17, 2020

Abstract: Semiconductor lasers (SLs) that are subject to delayed optical feedback and external optical injection have been demonstrated to perform information processing using the photonic reservoir computing paradigm. Optical injection or optical feedback can under some conditions induce bandwidth-enhanced operation, expanding their modulation response up to several tens of GHz. However, these conditions may not always result in the best performance for computational tasks, since the dynamical and nonlinear properties of the reservoir might change as well. Here we show that by using strong optical injection we can obtain an increased frequency response and a significant acceleration in the information processing capability of this nonlinear system, without loss of performance. Specifically, we demonstrate numerically that the sampling time of the photonic reservoir can be as small as 12 ps while preserving the same computational performance when compared to a much slower sampling rate. We also show that strong optical injection expands the reservoir's operating conditions for which we obtain improved task performance. The latter is validated experimentally for larger sampling times of 100 ps. The above attributes are demonstrated in a coherent optical communication decoding task.

***Corresponding author: Apostolos Argyris**, Instituto de Física Interdisciplinar y Sistemas Complejos IFISC (CSIC-UIB), Campus UIB, Palma de Mallorca, 07122, Spain,
E-mail: apostolos@ifisc.uib-csic.es. https://orcid.org/0000-0003-2847-7719
Irene Estébanez and Ingo Fischer: Instituto de Física Interdisciplinar y Sistemas Complejos IFISC (CSIC-UIB), Campus UIB, Palma de Mallorca, 07122, Spain, E-mail: irene@ifisc.uib-csic.es (I. Estébanez), ingo@ifisc.uib-csic.es (I. Fischer). https://orcid.org/0000-0002-0130-8774 (I. Estébanez). https://orcid.org/0000-0003-1881-9842 (I. Fischer)
Janek Schwind: Instituto de Física Interdisciplinar y Sistemas Complejos IFISC (CSIC-UIB), Campus UIB, Palma de Mallorca, 07122, Spain; Institute of Applied Physics, University of Münster, Münster, 48149, Germany, E-mail: janek@ifisc.uib-csic.es

Keywords: bandwidth enhancement; optical feedback; optical injection; photonic reservoir computing; semiconductor lasers.

1 Introduction

Reservoir computing has proven to be a powerful platform that can simplify the implementation of recurrent neural networks for versatile information processing tasks [1–3]. Time-delay reservoir computing (TDRC) has been a further simplified approach with minimal hardware requirements and energy-efficient designs [4]. Its ability for computation originates from the nonlinear transformation of the information to be processed onto a high-dimensional state space, assisted by the fading memory properties of the time-delayed reservoir. By exploiting the operating bandwidth of photonic systems and the hardware-efficient photonic topologies, one can target at high information processing speed [5–7]. This makes such photonic reservoir computers ideal candidates for analog processing of optical communication signals [8–10]. In the past, semiconductor lasers (SL) with time-delayed feedback have been used for generating broadband chaotic signals for applications such as chaotic encryption [11] and physical random number generation [12], by biasing the SL well above the lasing threshold. Moreover, such systems exhibited enhanced dynamical bandwidth emission in presence of an additional optical injection signal [13–18].

Here we consider a photonic reservoir computer based on a SL (response laser) with time-delayed optical feedback, while biasing the laser just below threshold. An optically injected signal from an external drive laser inserts the information to be processed by the reservoir. We show that the strength of this external optical injection, can be also used to modify the frequency response of the photonic reservoir. By adopting a strong injection condition and readjusting the operating conditions of the reservoir, we can significantly accelerate the information processing rate of a classification task while preserving the same performance. Nonlinear distortion compensation in fiber optic communications has been a challenging task for

many years. Depending on the considered approach, compensation might be applied on the transmitter side, along the optical link, or at the receiver side. It can be also implemented either in the optical or digital domain. Especially digital signal processing (DSP) algorithms – such as digital backpropagation [19], Volterra-based nonlinear equalizers [20], phase conjugation techniques [21], perturbation-based nonlinear compensation techniques [22], nonlinear Fourier transform [23], etc. – have been very efficient at dealing with fiber impairments. Lately, machine learning algorithms have been also contributing to the mitigation of fiber channel nonlinearities [24–26], including also hardware-based approaches [8–10]. Here we apply the proposed bandwidth enhanced operation of the TDRC approach, in a coherent fiber-optic transmission system, as a nonlinear distortion equalizer. We also validate the claim for information processing acceleration in a second benchmark test – the one-step-ahead Santa-Fe time-series prediction task – which is presented and discussed only in Supplementary material.

2 Materials and methods

2.1 Photonic reservoir with SL and time-delayed optical feedback

The structure of the photonic reservoir is presented schematically in Figure 1. We model the system numerically by using the adapted Lang-Kobayashi rate equations [27, 28], which include an additional optical injection term. The full model description and the relevant parameters' values are provided in Supplementary material. Several key parameters determine the dynamical properties of the photonic TDRC. These are linked to: (a) the reservoir: this includes the definition of the time delay of the optical feedback loop (τ), the feedback strength of the response laser described by the parameter r_c, the injection strength of the drive laser given by the parameter r_{inj} and the frequency detuning between the drive and the response laser $\Delta f = f_d - f_r$; (b) the information to be processed, which in our case is a modulation signal m on the drive laser's optical emission; and (c) the time-multiplexing characteristics that define certain properties of the reservoir: these include the number of the equidistant virtual nodes N that are defined within the physical time delay τ and their temporal separation θ that determines the properties of the transient states that will be used for the computing tasks.

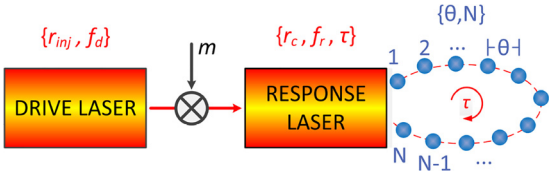

Figure 1: A photonic reservoir built with a SL subject to time-delayed optical feedback, with N virtual nodes defined by their equidistant time separation θ. The injected light that originates from the external drive (or injection) laser has a twofold function: to introduce the information to be processed by the reservoir through carrier modulation and to enhance the bandwidth response of the reservoir.

In principle, reservoir computers with shorter time delays can process the information faster, but allow the definition of less virtual nodes. Depending on the complexity of the nonlinear task that is addressed, more virtual nodes can be introduced by increasing the delay time τ – and slowing down the processing speed –, or by choosing a shorter time separation θ between virtual nodes. For reservoir computers that use the inertia of the transient responses to introduce coupling among the virtual nodes, the separation θ should be smaller than the response time T of the nonlinear node. However, θ should also not be chosen too small. In previous works with assorted computational tasks, a suitable time separation θ was found to be of the order of 0.2 T [4, 29, 30], ensuring that the nonlinear system exhibits a sufficiently large response to its input. In our study, we explore how to speed up the information processing by increasing the bandwidth response of the photonic reservoir. This will consequently allow reducing θ and ultimately use smaller delay times τ while keeping the number of virtual nodes of the reservoir constant. By controlling the strength of the optical injection carrier (r_{inj}), the reservoir's bandwidth response can be changed. We focus our investigation on two different levels of optical injection strength, a moderate injection with $r_{inj} = 0.4$ and a strong injection with $r_{inj} = 2$. For these two injection levels we study the performance of reservoirs that have two different virtual node separations: $\theta = 100$ ps and $\theta = 12$ ps. We evaluate and compare the performance in a parameter space which is defined by the physical quantities $\{r_c, \Delta f\}$. For our numerical modeling, we consider initially $N = 80$ along one time delay τ. This size of the reservoir provides a fair compromise between efficient computational performance and speed.

2.2 Computing task

The task we evaluate here originates from the optical communications field and targets on signal recovery after fiber transmission. In the recent past, we have demonstrated the potential of TDRC for signal processing in optical communication systems [8]. In that work we addressed a signal recovery task by using a direct detection scheme. Here we investigate the potential of the TDRC to process signals in a coherent-detection transmission scheme. Specifically, we consider a 180 km-long, coherent transmission system at 1550 nm with encoding rate of 28 GBd/s. The transmission path includes a dispersion compensating fiber just after the emitter, but no optical amplification at any stage. The transmission channel is simulated by the coupled nonlinear Schrödinger equations (CNLSE) [31]. An optical carrier is generated from a distributed feedback (DFB) SL. Two independent random binary streams are encoded in this carrier through a two-armed intensity-phase IQ Mach-Zehnder modulator (MZM) to form the quadrature phase shift keying (QPSK) optical signal. We simulate a dispersion compensating fiber (DCF) with appropriate length before transmission. At the end of the transmission link, a bandwidth-limited balanced photoreceiver is modeled by two p–i–n photodetectors with transimpedance gain (TIA) that include thermal and shot noise effects. Their frequency response has a cutoff at 0.8 of the data encoding rate. The coherent detector includes a DFB SL local oscillator which is

synchronized in frequency with the emitter laser. The two microwave branches of the balanced photoreceiver provide then the detected binary streams after transmission. Each stream is finally processed individually by the reservoir. The complete set of parameters used for the numerical simulation of the transmission system is provided in Supplementary material. The high launched power in the transmission channel causes high nonlinear signal distortion, but it also allows us to reach the 180 km distance with a signal to noise ratio of SNR = 10.5 dB for the detected signal.

2.3 Reservoir computing implementation

The detected signal from the coherent transmission system is introduced as a time-multiplexed signal at the input layer of the TDRC. More precisely, each binary pattern of information is represented by eight samples and is processed within one time delay τ of the reservoir. The information carried by these eight samples is expanded through interpolation over the number of virtual nodes N defined within the delay loop τ. In our consideration, when $N = 80$, each of the $N/8 = 10$ nodes receives the same input sample's value. In order to introduce a diversity of responses of the virtual nodes, the input is pre-processed (or masked) before entering into the reservoir. The mask $h(t)$ contains N input weights drawn from a random uniform distribution [0,1] and each virtual node is multiplied with one weight value which is preserved for the whole task. This mask represents a static connectivity matrix between the input information and the reservoir's virtual nodes. A visualization of the input sequence pre-processing is given in Supplementary material.

At the output layer of the TDRC, we consider the responses from 2000 binary patterns to train the system via an offline, standard, linear (ridge) regression algorithm with ridge parameter $\lambda = 0.01$ [32]. The calculated weights from the training procedure are then used to evaluate the binary values of 4000 patterns from independent test sets of this task. The error rate of the data recovery is calculated by comparing the computed binary value with the binary value that was initially encoded at the transmission system, via the logarithmic bit error rate log (BER).

We have shown in the past [8] that for such kind of tasks, the identification of a binary pattern depends also on its neighboring patterns. The number of neighboring patterns that should be taken into account depends on the mechanisms that disperse information to subsequent time frames. Here, we consider up to 10 neighboring patterns, in addition to the current pattern of the investigated time frame. This is rather a small number, compared to [8, 9] since, in this task, chromatic dispersion compensation is applied before fiber transmission. Thus, the nonlinear distortions that interfere with neighboring bit patterns do not extend very far in time. For all the investigations in this work, we determine the number of neighbors which leads to the minimum error rate. In almost all cases, this number lies between 5 and 9. This also means that the total number of virtual nodes' responses that participate in the training process and the classification task will be N times the number of patterns. For comparison reasons, we evaluated the same computing algorithm to the detected signal from the transmission system, without passing through the photonic reservoir. In this case, we obtain a decoding performance with as low as $\log(\mathrm{BER})_{REF} = -1.6$. This error rate is well above the hard decision, forward error correction (HD-FEC) BER requirement for error-free decoding [33], which is equal to $\log(\mathrm{BER})_{HD-FEC} = -2.42$.

3 Results

3.1 Bandwidth-enhanced reservoir operation

We start by characterizing the bandwidth enhancement through optical injection in our system, in which the response laser is biased (I_r) just below its threshold current. The laser emission is then triggered by the optical feedback and optical injection terms. We define as the response bandwidth of the reservoir the frequency interval between DC (while excluding the DC component) and the frequency which contains 80% of the total power spectral density of the emitted signal. We consider a photonic reservoir with a delay of $\tau = N{\cdot}\theta = 80{\cdot}12$ ps = 960 ps, where $N = 80$ and $\theta = 12$ ps. Random input noise, chosen from a uniform distribution, is fed into the photonic reservoir via the optical injection carrier for every iteration step of the integration method (1 ps). The frequency response that is obtained in the $\{r_c, \Delta f\}$ parameter space, for the two optical injection conditions ($r_{inj} = 0.4$ and $r_{inj} = 2$), is shown in Figure 2A,B, respectively. A first observation is that the frequency response of the reservoir is systematically enhanced for the strong injection condition, compared to the moderate injection case. This enhancement is found within most of the investigated parameter region $\{r_c,\ \Delta f\} \in \{[0, 0.2],\ [-45\ \mathrm{GHz}, 60\ \mathrm{GHz}]\}$ and ranges from a few GHz to more than 10 GHz. This is an effect that can potentially lead to boost the information processing rate of our photonic reservoir. However, the reservoir computing performance relies also on the dynamical nonlinear effects that change with injection strength, frequency detuning and feedback strength. The response laser – by interacting with the injected signal, as well as with its own time-delayed emission – is an active system, exhibiting several dynamical phenomena. Thus, its frequency response is not only a filtering process of the input signal. For example, in the case of moderate injection (Figure 2A), the regions in the parameter space with strong frequency detuning ($|\Delta f| > 50$ GHz) and strong optical feedback ($r_c > 0.1$) show an effective reduction of the system's frequency response. The latter originates from the onset of coherence collapse of the response laser [34]; in these regimes chaotic emission is found and information processing tasks cannot be executed efficiently. A similar chaotic emission is expected also for the case of strong injection (Figure 2B), but at higher values of the feedback parameter than the ones recorded here. The bandwidth enhancement depends also on the injection locking conditions of the reservoir laser to the injected signal. For complete injection locking, this

influence is observed for negative frequency detuning Δf [27, 28]. As the optical injection becomes stronger, the frequency detuning $|\Delta f|$ for which we find complete injection locking shifts to higher negative values. The boundaries of complete injection locking are observed where the bandwidth response shows a local minimum: around –18 GHz for the moderate injection case (Figure 2A) and around –47 GHz for strong injection case (Figure 2B).

Although several operating conditions may lead to similar bandwidth response, this can originate from different spectral profiles. An example is given in Figure 2C. We select two operating conditions in the $\{r_c, \Delta f\}$ parameter space: (i) {0.05, 0 GHz} and (ii) {0.07, 33 GHz}, for the two investigated optical injection conditions ($r_{inj} = 0.4$ and $r_{inj} = 2$). When the frequency detuning is small or zero, as in case (i), there is a continuous low-pass nonlinear response of the reservoir to the injected signal. But as the frequency detuning becomes larger, as in case (ii), moderate injection conditions ($r_{inj} = 0.4$) allow rather a band-pass nonlinear reservoir response. This shows only low frequency components, combined with a response region around a peak frequency that depends on Δf and r_{inj}. All frequency components between these two regimes are strongly suppressed. In contrast, when increasing the optical injection ($r_{inj} = 2$), the previously suppressed frequency components contribute much more now. In both cases (i) and (ii), strong injection leads to a broader spectrum, with much higher power spectral density of all frequency components. This broadband operation is expected to contribute positively to the computation tasks. We find equivalent dependencies when considering larger time delays and larger virtual node separation θ of the reservoir, e. g., for $\tau = N{\cdot}\theta = 80{\cdot}100$ ps = 8 ns.

In section Photonic reservoir with SL and time-delayed optical feedback we discussed the conditions that the time separation θ of the virtual nodes must fulfill, with respect to the response time T of the nonlinear node. If the nonlinear node was a solitary laser, its response time would be associated with the relaxation oscillation frequency. However, the dynamical photonic reservoir response is influenced by various system properties. The response laser is biased below threshold and its emission is induced only in presence of the external perturbations, i. e., the optical feedback and the optical injection. Figure 2A,B illustrate that the frequency response depends on the interaction conditions between the nonlinear node and the perturbations. Thus, it would be inaccurate to assign a unique response time T to this system. One has to identify those conditions that will lead to an appropriate ratio of response time T and virtual node separation θ, in order to address a certain computational task [4, 29, 30] But even then, the nonlinear transformation of the TDRC system will finally determine the overall computation performance.

3.2 Computing task performance

Favorable operating conditions of the photonic reservoir should combine – besides the sufficient bandwidth response – other important attributes for computing, such as fading memory and consistent nonlinear input/output signal transformation [35]. When considering a photonic TDRC, its dynamical response to an input signal determines the nonlinear transformation and eventually the computing performance of the associated computational task. As discussed in section Materials and methods, the smaller the virtual node separation θ is, the faster the information processing can be, if the nonlinear responses have sufficiently large amplitude. Here, we identify those conditions that result in bandwidth enhanced operation and we study whether we can benefit from faster transient states and smaller virtual node separations θ, without losing computational performance.

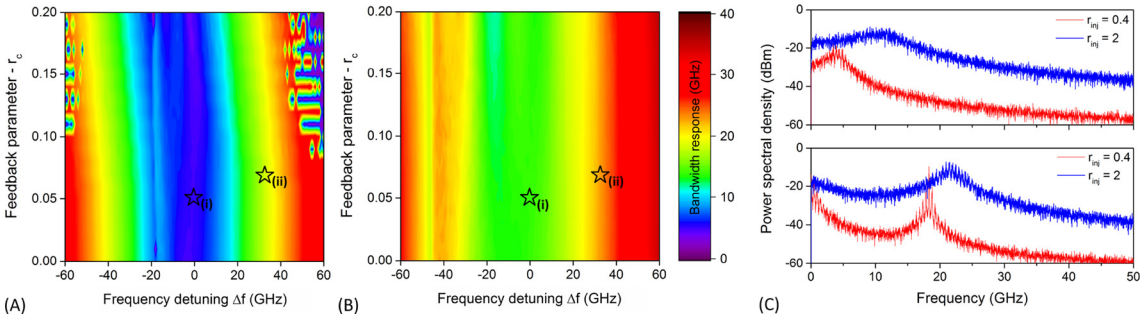

Figure 2: Frequency response of the photonic reservoir for (A) moderate ($r_{inj} = 0.4$) and (B) strong ($r_{inj} = 2$) optical injection conditions, in the $\{r_c, \Delta f\}$ parameter space. (C) Frequency response profiles for moderate ($r_{inj} = 0.4$) and strong ($r_{inj} = 2$) optical injection, for two operating conditions of the photonic reservoir in the $\{r_c, \Delta f\}$ parameter space: (i) {0.05, 0 *GHz*} and (ii) {0.07, 33 *GHz*}. These conditions are noted with star shapes in panels (A) and (B).

3.2.1 Slow transient operation

Initially we consider the case of a photonic TDRC with large virtual node separation of θ = 100 ps (τ = 8 ns) and we evaluate its efficiency to recover the encoded binary sequences for the transmission task described in section Materials and methods. This is obtained via a high-resolution $\{r_c,\ \Delta f\}$ parameter scan, for the two cases of optical injection (r_{inj} = 0.4 and r_{inj} = 2). The results are shown in Figure 3. The conditions for best performance for moderate (Figure 3A) and strong (Figure 3B) optical injection are located in different regions of this parameter space. Nevertheless, the best obtained performance is similar for both cases and corresponds to a logarithmic bit error rate as low as log(BER) = −2.9. This means that by using bandwidth enhancement techniques we can maintain a similar computing performance at higher processing speed. However, strong optical injection conditions define a wider parameter space to obtain the lowest error rates. Finally, the optical feedback cavity with τ = 8 ns (θ = 100 ps) is at the boundary of the short-long cavity regime [27, 28, 38]. Thus, the dynamical response of the reservoir is only slightly affected by the optical feedback phase.

3.2.2 Fast transient operation

When the photonic TDRC is realized with the smaller virtual node separation (θ = 12 ps), an additional consideration must be taken into account for achieving the highest computational performance. The time delay in this case (τ = 960 ps) lies in the short cavity regime [27, 28, 36–38]. The phase condition of the delayed feedback signal plays now a significant role in the dynamical behavior of the system. Thus, the phase of the optical feedback loop is an additional parameter that enters into the considered parameter space.

Therefore, we evaluate the same signal recovery task for θ = 12 ps, but in an extended three-dimensional $\{r_c,\ \Delta f,\ \varphi\}$ parameter space, that also includes the phase dependency of the feedback cavity. The error-rate comparison for the two optical injection cases is shown in Figure 4. These two-dimensional mapping graphs are obtained after a scan of the feedback phase value in the range $[0, 2\pi]$, for each $\{r_c, \Delta f\}$ condition. For moderate optical injection (Figure 4A), the minimum error rate has a value of log(*BER*) = −2.24 and is only found for a very small range of operating conditions around $\{r_c = 0.03, \Delta f = 8$ GHz$\}$. For this operating condition, the dynamical bandwidth of the reservoir is only 7.1 GHz; thus, the limited frequency response of the reservoir cannot provide sufficiently fast transient responses, affecting the overall computing performance. Such conditions are not adequate to provide an error-free decoding of the examined

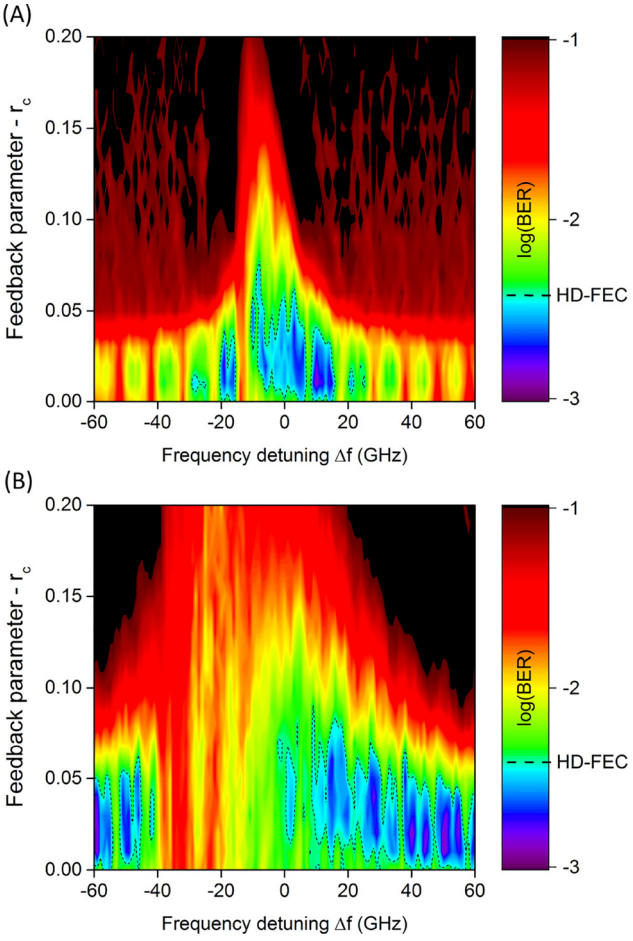

Figure 3: BER performance of data recovery after RC post-processing in the $\{r_c, \Delta f\}$ parameter space of a reservoir with large virtual node separation (θ = 100 ps), for (A) moderate (r_{inj} = 0.4) and (B) strong (r_{inj} = 2) optical injection. Black dashed line includes the areas with log(*BER*) < log(*BER*)$_{HD-FEC}$ = −2.42.

task, through additional HD-FEC encoding. In contrast, by considering strong optical injection conditions, the bandwidth enhancement allows the generation of faster transient states (Figure 4B). The minimum log (BER) value obtained is improved now to −2.9, as found for the operating condition ($\{r_c = 0.07, \Delta f = 33$ GHz$\}$). The corresponding bandwidth response is now 22.9 GHz, showing a significant increase of 15.8 GHz compared to moderate injection condition. Moreover, an error-free data recovery, which can be obtained when log(*BER*) < log(*BER*)$_{HD-FEC}$ can be found for several and wider regions of the parameter space, as indicated by the black-dashed areas in Figure 4B. This finding relaxes significantly the tolerance of the operating conditions for the photonic reservoir and facilitates the identification of the set of parameters for the best performance. Under both injection conditions, the phase φ of optical feedback is an important parameter for the dynamical response of the photonic

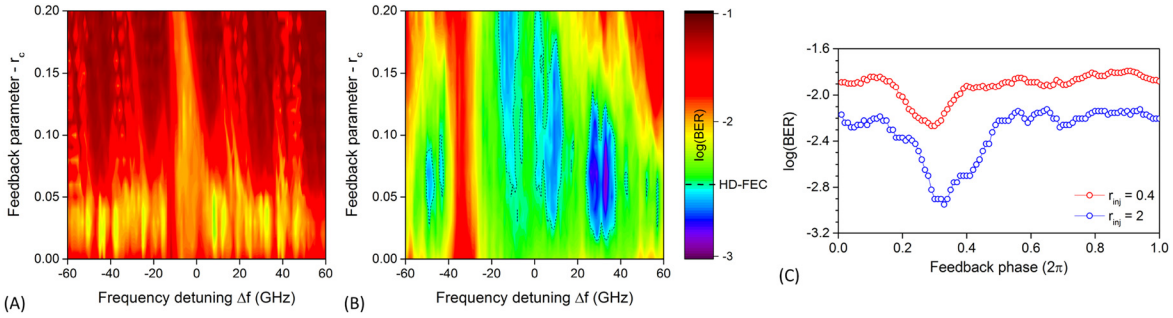

Figure 4: BER performance of data recovery after RC post-processing in the $\{r_c,\ \Delta f,\ \varphi\}$ parameter space of a reservoir with small virtual node separation (θ = 12 ps), for (A) moderate (r_{inj} = 0.4) and (B) strong (r_{inj} = 2) optical injection. The black dashed line indicates the areas with log(*BER*) < log(*BER*)$_{HD-FEC}$ = −2.42. (C) Optical feedback phase versus error rate performance, for the best operating conditions of (A) (red circles) and (B) (blue circles).

reservoir. In Figure 4C we show the phase dependence of the error rate performance, for the best operating conditions of (A) (red circles) and (B) (blue circles). Finally, we validate the importance of the system's frequency response and its contribution to the computational performance, by applying a low-pass filter to the reservoir's response for the strong injection scenario. We select a cutoff frequency that results in a response bandwidth equal to the one obtained for the best performance at moderate injection (7.1 GHz). We repeat the evaluation for the best conditions identified in Figure 4B ($\{r_c$ = 0.07, Δf = 33 GHz$\}$) and we obtain a data recovery performance similar to the moderate injection case, with log(*BER*) = −2.12. This illustrates the importance of the bandwidth enhancement when considering smaller virtual node separations to speed up the computation.

4 Reservoir optimization

In the previous parts of section Results, our investigation was focused on the physical properties and operating conditions of the photonic reservoir. Two other system variables that can be used to further optimize the TDRC performance are the number of virtual nodes *N* and the masking sequence that is used for the input connectivity assignment to the reservoir[39–41]. For the best operating condition of the bandwidth-enhanced operation (r_{inj} = 2), as obtained from Figure 4A,B for the two different θ values, we show the task performance dependence on different reservoir sizes *N* and for 100 different random masking sequences. The evaluation results are presented in Figure 5, showing several clear trends. First, the masking sequence can play a decisive role on the task performance. The height of the bars in Figure 5 indicates the minimum and maximum error rate performance for the different masking sequences, which has been analyzed for the two injection conditions. The large bar height implies that an optimization procedure needs to be included in the pre-selection of the connectivity input pattern for the reservoir. Second, a reservoir that includes a larger number of virtual nodes improves the task performance. This comes, however, at the expense of a slower processing per unit information, since the total time delay of the photonic reservoir increases. Finally, strong injection conditions always allow the TDRC system to reach lower error rates, compared to weaker injection, for a given reservoir size.

5 Experimental validation in slow transient operation

Based on the numerical analysis presented in the previous section, we can make the following two claims: (i) for slow

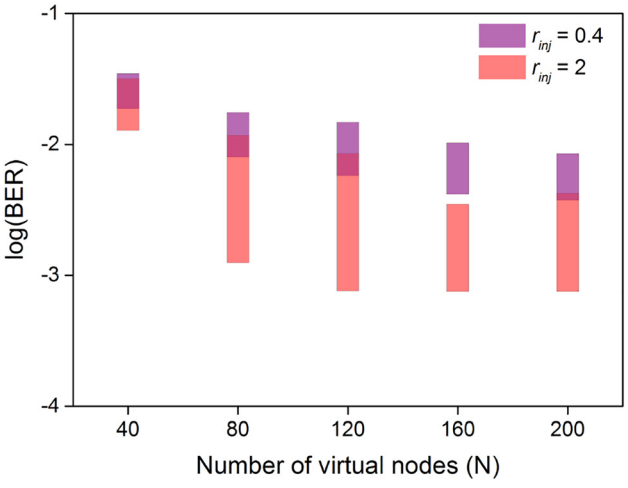

Figure 5: BER performance of data recovery after RC post-processing for the optimal $\{r_c, \Delta f\}$ parameters, for small virtual node separation (θ = 12 ps) of the reservoir and for moderate (r_{inj} = 0.4) and strong (r_{inj} = 2) optical injection, versus the number of virtual nodes *N*. One-hundred different masking sequences for the reservoir input connectivity have been tested.

transient operation, strong injection increases the parameter region in which we achieve better performance. (ii) for fast transient operation, the combination of strong injection and bandwidth enhanced operation is required to reach the best performance. We validate our first claim experimentally, by implementing a photonic reservoir to address the task described in section Computing task. To this end, we had to slightly adjust the transmission length of the communication system. In particular, we reduced that slightly to 170 km, to compensate for additional noise sources we have in the experimental implementation. The reservoir is an optical fiber-based implementation of the concept presented in Figure 1. It consists of a long cavity time delay of $\tau = 16.8$ ns, with a virtual node separation of $\theta = 100$ ps. This means that we can define 168 virtual nodes along the fiber loop, from which we use only the first $N = 80$ virtual node responses to process the input information. For this cavity length, there is no dependence on the optical feedback phase. The classification algorithm we apply is also the same as described in section Computing task. It is implemented offline. All relevant details for the experimental configuration and corresponding parameters can be found in Supplementary material.

Figure 6 depicts the error rate performance of the data recovery task with the TDRC, when using the experimental photonic reservoir. The characterization has been performed in dependence on the frequency detuning Δf, for two different feedback ratios ($r_c = 0.019$ and $r_c = 0.035$) and for moderate ($P_{inj} = 0.125$ mW, Figure 6A) and strong ($P_{inj} = 0.5$ mW, Figure 6B) optical injection. Strong optical injection yields a lower error rate for many operating conditions of the reservoir. However, we find the minimum error rate to be the same for both moderate and strong injection ($\log(BER) = -2.8$). The overall performance behavior is in agreement with our numerical results shown in Figure 3.

The experimental validation of the system's behavior in the fast transient operation is still an open challenge for the future. The proposed node separation ($\theta = 12$ ps) lies at the technological limit of the supporting instrumentation, such as the waveform generators which are commonly used to introduce the information to be processed into the photonic system. Such small θ values are desirable since they allow the definition of a larger number of virtual nodes in experimental implementations of photonic integrated circuits, where the time delay is limited. In such platforms it is feasible to control the phase of the delay feedback field, and hence the dynamical operation of such devices, as it has been shown in the past [42, 43].

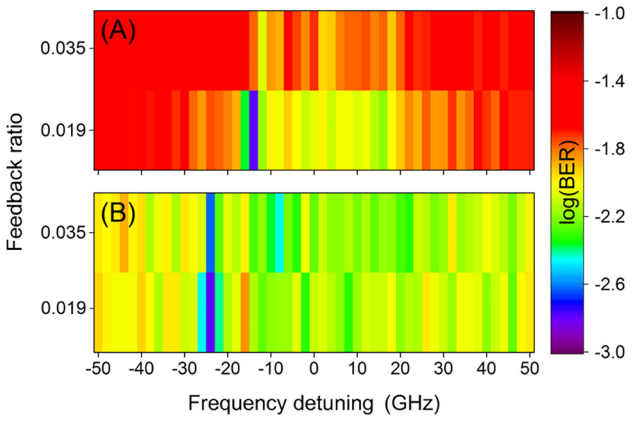

Figure 6: BER performance of data recovery after post-processing with an experimental photonic reservoir, for a slow transient reservoir operation ($\theta = 100$ ps), versus frequency detuning Δf, for two different feedback ratios ($r_c = 0.019$ and $r_c = 0.035$) and for (A) moderate ($P_{inj} = 0.125$ mW) and (B) strong ($P_{inj} = 0.5$ mW) optical injection.

6 Discussion

In this study, we demonstrated numerically the potential of bandwidth-enhanced operation for photonic TDRC to speed up their computation without sacrificing performance. Bandwidth enhancement is a necessary condition to generate fast transient states with sufficient amplitude; however, it is not a sufficient condition to achieve good reservoir computing performance. Our approach to achieve both attributes is by varying the strength and the frequency detuning of the optical carrier that introduces the information to be processed by the TDRC. For strong optical injection and properly chosen frequency detuning, feedback strength and feedback phase, we enable the use of virtual node separations of only 12 ps – the shortest reported so far – for successfully implementing an optical communication signal recovery task. While we have experimentally demonstrated that strong optical injection increases the tolerance of selecting the appropriate operating conditions of the TDRC, the numerical findings of this study provide a roadmap for implementing experimentally the bandwidth enhanced approach in the near future.

Acknowledgment: This work was supported by MINECO (Spain), through project TEC2016-80063-C3 (AEI/FEDER, UE) and by the Spanish State Research Agency, through the Severo Ochoa and María de Maeztu Program for Centers and Units of Excellence in R&D (MDM-2017-0711). The work of Dr. A. Argyris was supported by the Conselleria d'Innovació, Recerca i Turisme del Govern de les Illes Balears and the European Social Fund.

Author contribution: All the authors have accepted responsibility for the entire content of this submitted manuscript and approved submission.
Employment or leadership: None declared.
Honorarium: None declared.
Conflict of interest statement: The authors declare no conflicts of interest regarding this article.

References

[1] H. Jaeger, *The "echo state" Approach to Analysing and Training Recurrent Neural Networks*, German National Research Center for Information Technology, 2001, GMD Report 148.
[2] W. Maass, T. Natschläger, and H. Markram, "Real-time computing without stable states: a new framework for neural computation based on perturbations," *Neural Comput.*, vol. 14, no. 11, pp. 2531–2560, 2002.
[3] H. Jaeger, and H. Haas, "Harnessing nonlinearity: predicting chaotic systems and saving energy in wireless communication," *Science*, vol. 304, pp. 78–80, 2004.
[4] L. Appeltant, M. C. Soriano, G. Van der Sande, et al., "Information processing using a single dynamical node as complex system," *Nat. Commun.*, vol. 2, p. 468, 2011.
[5] Y. Paquot, F. Duport, A. Smerieri, et al., "Optoelectronic reservoir computing," *Sci. Rep.*, vol. 2, no. 1, p. 287, 2012.
[6] L. Larger, M. C. Soriano, D. Brunner, et al., "Photonic information processing beyond Turing: an optoelectronic implementation of reservoir computing," *Opt. Expr.*, vol. 20, no. 3, pp. 3241–3249, 2012.
[7] D. Brunner, M. C. Soriano, C. R. Mirasso, and I. Fischer, "Parallel photonic information processing at gigabyte per second data rates using transient states," *Nat. Commun.*, vol. 4, p. 1364, 2013.
[8] A. Argyris, J. Bueno, and I. Fischer, "Photonic machine learning implementation for signal recovery in optical communications," *Sci. Rep.*, vol. 8, no. 1, p. 8487, 2018.
[9] A. Argyris, J. Bueno, and I. Fischer, "PAM-4 transmission at 1550 nm using photonic reservoir computing post-processing," *IEEE Access*, vol. 7, Art no. 37017, 2019, https://doi.org/10.1109/ACCESS.2019.2905422.
[10] M. Sorokina, S. Sergeyev, and S. Turitsyn, "Fiber echo state network analogue for high-bandwidth dual-quadrature signal processing," *Opt .Expr.*, vol. 27, no. 3, pp. 2387–2395, 2019.
[11] A. Argyris, D. Syvridis, L. Larger, et al., "Chaos-based communications at high bit rates using commercial fibre-optic links," *Nature*, vol. 438, pp. 343–346, 2005.
[12] A. Uchida, K. Amano, and M. Inoue, "Fast physical random bit generation with chaotic semiconductor lasers," *Nat. Photon*, vol. 2, p. 728, 2008.
[13] R. Lang, and K. Kobayashi, "External optical feedback effects on semiconductor injection laser properties," *IEEE J. Quantum Electron*, vol. QE-16, pp. 347–355, 1980.
[14] T. B. Simpson, J. M. Liu, and A. Gavrielides, "Bandwidth enhancement and broadband noise reduction in injection-locked semiconductor lasers," *IEEE Phot. Technol. Lett.*, vol. 7, no. 7, pp. 709–711, 1995.
[15] J. Wang, M. K. Haldar, L. Li, and F. V. C. Mendis, "Enhancement of modulation bandwidth of laser diodes by injection locking," *IEEE Phot. Technol. Lett.*, vol. 8, no. 1, p. 34, 1996.
[16] J. M. Liu, H. F. Chen, X. J. Meng, and T. B. Simpson, "Modulation bandwidth, noise, and stability of a semiconductor laser subject to strong injection locking," *IEEE Phot. Technol. Lett.*, vol. 9, 10, pp. 1325–1327, 1997.
[17] H. Someya, I. Oowada, H. Okumura, T. Kida, and A. Uchida, "Synchronization of bandwidth-enhanced chaos in semiconductor lasers with optical feedback and injection," *Opt. Expr.*, vol. 17, pp. 19536–19543, 2009.
[18] K. Kanno, A. Uchida, and M. Bunsen, "Complexity and bandwidth enhancement in unidirectionally coupled semiconductor lasers with time-delayed optical feedback," *Phys. Rev. E*, vol. 93, no. 3, 2016, Art no. 032206, https://doi.org/10.1103/PhysRevE.93.032206.
[19] E. Ip, and J. M. Kahn, "Compensation of dispersion and nonlinear impairments using digital back propagation," *IEEE OSA J. Lightw. Technol.*, vol. 26, no. 20, pp. 3416–3425, 2008.
[20] F. P. Guiomar, J. D. Reis, A. L. Teixeira, and A. N. Pinto, "Digital postcompensation using Volterra series transfer function," *IEEE Photon Technol. Lett.*, vol. 23, no. 19, p. 8660, 2011.
[21] X. Liu, A. R. Chraplyvy, P. J. Winzer, R. W. Tkach, and S. Chandrasekhar, "Phase-conjugated twin waves for communication beyond the Kerr nonlinearity limit," *Nat. Photon*, vol. 7, pp. 560–568, 2013.
[22] X. Liang, S. Kumar, J. Shao, M.Malekiha, and D. V.Plant, "Digital compensation of cross-phase modulation distortions using perturbation technique for dispersion-managed fiber-optic systems," *Opt. Expr.*, vol. 22, no. 17, Art no. 20634, 2014, https://doi.org/10.1364/OE.22.020634.
[23] J. E. Prilepsky, S. A. Derevyanko, K. J. Blow, I. Gabitov, and S. K. Turitsyn, "Nonlinear inverse synthesis and eigenvalue division multiplexing in optical fiber channels," *Phys. Rev. Lett.*, vol. 113, no. 1, Art no. 13901, 2014, https://doi.org/10.1103/PhysRevLett.113.013901.
[24] M. A. Jarajreh, E. Giacoumidis, I. Aldaya, et al., "Artificial neural network nonlinear equalizer for coherent optical OFDM," *IEEE Photon Technol. Lett.*, vol. 27, no. 4, pp. 387–390, 2015.
[25] D. Wang, M. Zhang, M. Fu, et al., "Nonlinearity mitigation using a machine learning detector based on k-nearest neighbors," *IEEE Photon Technol. Lett.*, vol. 28, no. 19, pp. 2102–2105, 2016.
[26] T. Nguyen, S. Mhatli, E. Giacoumidis, L. Van Compernolle, M. Wuilpart, and P. Mgret, "Fiber nonlinearity equalizer based on support vector classification for coherent optical OFDM," *IEEE Photon J.*, vol. 8, no. 2, Art no. 7802009, 2016, https://doi.org/10.1109/JPHOT.2016.2528886.
[27] K. Petermann, "External optical feedback phenomena in semiconductor lasers," *IEEE J. Sel. Top. Quantum Electron*, vol. 1, no. 2, pp. 480–489, 1995.
[28] J. Ohtsubo, *Semiconductor Lasers: Stability, Instability and Chaos*, 4th ed. Berlin, Heildelberg, Germany, Springer-Verlag, 2017.
[29] M. C. Soriano, S. Ortín, L. Keuninckx, et al., "Delay-based reservoir computing: noise effects in a combined analog and digital implementation," *IEEE Trans. Neur. Net. Learn Sys.*, vol. 26, no. 2, pp. 388–393, 2014.
[30] S. Ortín, and L. Pesquera, "Delay-based reservoir computing: tackling performance degradation due to system response time," *Opt. Lett.*, vol. 45, no. 4, pp. 905–908, 2020.
[31] G. P. Agrawal, *Fibre-Optic Communication Systems*, 4th ed. New York, NY, USA, Wiley-Blackwell, 2010.
[32] A. E. Hoerl, and R. W. Kennard, "Ridge regression: applications to nonorthogonal problems," *Technometrics*, vol. 12, no. 1, p. 55, 1970.

[33] G. Tzimpragos, C. Kachris, I. B. Djordjevic, M. Cvijetic, D. Soudris, and I. Tomkos, "A survey on FEC codes for 100G and beyond optical networks," *IEEE Commun. Surv. Tutor*, vol. 18, no. 1, pp. 209–221, 2016.

[34] M. C. Soriano, J. García-Ojalvo, C. R. Mirasso, I. Fischer, "Complex photonics: dynamics and applications of delay-coupled semiconductors lasers," *Rev. Mod. Phys.*, vol. 85, Art no. 421, 2013, https://doi.org/10.1103/RevModPhys.85.421.

[35] J. Bueno, D. Brunner, M. C. Soriano, I. Fischer, "Conditions for reservoir computing performance using semiconductor lasers with delayed optical feedback," *Opt. Expr.*, vol. 25, no. 3, pp. 2401–2412, 2017.

[36] T. Heil, I. Fischer, W. Elsäßer, and A. Gavrielides, "Dynamics of semiconductor lasers subject to delayed optical feedback: the short cavity regime," *Phys. Rev. Lett.*, vol. 87, Art no. 243901, 2001, https://doi.org/10.1103/PhysRevLett.87.243901.

[37] O. Ushakov, S. Bauer, O. Brox, H. J. Wünsche, and F. Henneberger, "Self-organization in semiconductor lasers with ultrashort optical feedback," *Phys. Rev. Lett.*, vol. 92, Art no. 043902, 2004, https://doi.org/10.1103/PhysRevLett.92.043902.

[38] D. M. Kane, and K. A. Shore, *Unlocking Dynamical Diversity*, 1st ed. West Sussex, England, Wiley, 2005.

[39] L. Appeltant, G. Van der Sande, J. Danckaert, and I. Fischer, "Constructing optimized binary masks for reservoir computing with delay systems," *Sci. Rep.*, vol. 4, Art no. 3629, 2014, https://doi.org/10.1038/srep03629.

[40] B. Schneider, J. Dambre, and P. Bienstman, "Using digital masks to enhance the bandwidth tolerance and improve the performance of on-chip reservoir computing systems," *IEEE Trans. Neur. Net. Learn Sys.*, vol. 27, no. 12, pp. 2748–2753, 2015.

[41] Y. Kuriki, J. Nakayama, K. Takano, and A. Uchida, "Impact of input mask signals on delay-based photonic reservoir computing with semiconductor lasers," *Opt. Expr.*, vol. 26, Art no. 5777, 2018, https://doi.org/10.1364/OE.26.005777.

[42] A. Argyris, M. Hamacher, K. E. Chlouverakis, A. Bogris, and D. Syvridis, "Photonic integrated device for chaos applications in communications," *Phys. Rev. Lett.*, vol. 100, Art no. 194101, 2008, https://doi.org/10.1103/PhysRevLett.100.194101.

[43] K. E. Chlouverakis, A. Argyris, A. Bogris, and D. Syvridis, "Hurst exponents and cyclic scenarios in a photonic integrated circuit," *Phys. Rev. E*, vol. 78, Art no. 066215, 2008, https://doi.org/10.1103/PhysRevE.78.066215.

Supplementary material: The online version of this article offers supplementary material (https://doi.org/10.1515/nanoph-2020-0184).